Dalton Transactions

Accepted Manuscript

ROYAL SOCIETY OF CHEMISTRY

www.rsc.org/dalton

Journal Name

RSCPublishing

ARTICLE

Dimeric 1,3-propanediaminetetraacetato lanthanides as the precursors of catalysts for the oxidative coupling of methane

Cite this: DOI: 10.1039/x0xx00000x

Received 00th January 2013,
Accepted 00th January 2013

DOI: 10.1039/x0xx00000x

www.rsc.org/

Mao-Long Chen, Yu-Hui Hou, Wen-Sheng Xia, Wei-Zheng Weng, Ze-Xing Cao*, Zhao-Hui Zhou*, Hui-Lin Wan

In neutral solution, dimeric 1,3-propanediaminetetraacetato lanthanides $(NH_4)_2[Ln_2(1,3\text{-pdta})_2(H_2O)_4]\cdot 8H_2O$ [Ln = La, **1**; Ce, **2**] and $K_2[Ln_2(1,3\text{-pdta})_2(H_2O)_4]\cdot 11H_2O$ [Ln = La, **3**; Ce, **4**] (1,3-H_4pdta = 1,3-propanediaminetetraacetic acid, $C_{11}H_{18}N_2O_8$) were isolated at high yields. Reaction of excess strontium nitrate with **1** resulted in the formation of a two dimensional coordination polymer $[La_2(1,3\text{-pdta})_2(H_2O)_4]_n\cdot[Sr_2(H_2O)_6]_n\cdot[La_2(1,3\text{-pdta})_2(H_2O)_2]_n\cdot 18nH_2O$ (**5**) at 70 °C. Complexes **1**−**4** show a similar central molecular structure. The lanthanide ions are coordinated by two nitrogen atoms, four carboxy oxygen atoms from one 1,3-pdta ligand, two from the neighboring 1,3-pdta ligand forming a four-membered ring and two water molecules. Complex **5** has two kinds of dimeric lanthanum unit and extends into a 2D coordination polymer through strontium ions and bridged oxygen atoms, and forms a fourteen membered ring linked by oxygen atoms from carboxy groups of pdta. **1**−**4** are soluble in water. The $^{13}C\{^1H\}$ NMR experiments for complex **1** were tested in solution. Thermal products from **1** and **5** show good catalytic activities for oxidative coupling reaction of methane (OCM). The conversion of methane and selectivity to C_2 reached to 29.7% and 51.7% at 750 °C for the product of **5**. From TGA, XRD and SEM analyses, the thermal products from **1** and **5** are in rod- and poly-shaped, which are assigned as lanthanum oxocarbonate and a mixture of La_2O_3, $SrCO_3$ and $La_2O_2CO_3$ for **1** and **5** respectively. The precursor method is favorable for the formation of regular shaped mixed oxides.

Introduction

Recently, lanthanide coordination complexes have attracted increasing attention because of their interesting properties such as magnetism,[1] optical properties,[2] and use as complexing agents in the separation of lanthanide cations,[3] contrast agents in magnetic resonance imaging,[4] and precursors for the syntheses of nanoparticles.[5] Lanthanide oxides-based and/or doped nanoparticles represent an interesting investigation field, which can be used as catalysts and supports for noble metal catalysts.[6] For example, lanthanum oxide finds its applications in solid oxide fuel cells and oxidative coupling of methane (OCM).[7] Metal oxides can be synthesized in several ways such as: sol–gel,[8] carbonate,[9] templates,[10] homogeneous precipitation,[11] thermal treatments of the precursors of coordination complexes,[12] etc. Among them, the thermal treatment of precursor method is attractive, since it consists of a moderate calcinated temperature with explicit composition, yielding high purity oxides. In general, 1,3-propanediaminetetraacetic acid {1,3-H_4pdta = $CH_2[CH_2N(CH_2CO_2H)_2]_2$} which is a edta-like ligand {edta = $[CH_2N(CH_2CO_2H)_2]_2$} is tetrabasic acid with eight potential O-donor and two N-donor atoms. Comparing with transition metals, lanthanide ions have high coordination number (CN) and coordination flexibility. Combination of 1,3-pdta and high CN of lanthanide might be expected to isolate different sorts of lanthanide complexes, which can be used as precursors in the thermal treatment processing. In previous paper, we have reported an interesting metal-organic framework (MOF) structure constructed by lanthanum and 1,3-pdta, which demonstrated a potential use for low-pressure desalination.[13] Herein, four dimeric hydrated 1,3-propanediaminetetraacetato lanthanides $(NH_4)_2[Ln_2(1,3\text{-pdta})_2(H_2O)_4]\cdot 8H_2O$ [Ln = La, **1**; Ce, **2**] and $K_2[Ln_2(1,3\text{-pdta})_2(H_2O)_4]\cdot 11H_2O$ [Ln = La, **3**; Ce, **4**] were isolated in high yields. With excess strontium nitrate, a two dimensional coordination polymer $[La_2(1,3\text{-pdta})_2(H_2O)_4]_n\cdot[Sr_2(H_2O)_6]_n\cdot[La_2(1,3\text{-pdta})_2(H_2O)_2]_n\cdot 18nH_2O$ (**5**) was isolated from **1**. The thermal analysis of **1** and **5** were investigated, and their thermal decomposition products show good catalytic activities to oxidative coupling of methane.

Experimental

Materials and instrumentation

All chemicals were of analytical or reagent-grade purity and used as received. The pH value was measured by potentiometric method with a PHB-8 digital pH meter. Elemental analyses (C, H, N) were performed by EA1110 elemental analyzer. Infrared spectra were recorded as KBr disks and as mulls in Nujol with a Nicolet 330 FT-IR spectrophotometer. SEM images were recorded on HITACHI S-4800 electron microscope. Thermogravimetric analysis were recorded on SDT-Q600 thermal analyzer, under an air flow of 100 mL·min^{-1} at a heating rate of 10 °C·min^{-1}. Solution $^{13}C\{^1H\}$ NMR spectra were recorded in D_2O on a Bruker AV 400 M NMR spectrometer using DSS (sodium 2,2-dimethyl-2-silapentane-5-sulfonate) as the internal reference. Powder X-ray diffraction (XRD) data were collected using monochromated Cu Kα radiation on a Phillips X'Pert diffractometer.

Synthesis

Preparations of dimeric $(NH_4)_2[La_2(1,3\text{-pdta})_2(H_2O)_4]\cdot 8H_2O$ (1) and $(NH_4)_2[Ce_2(1,3\text{-pdta})_2(H_2O)_4]\cdot 8H_2O$ (2)

$LaCl_3\cdot 7H_2O$ (0.74 g, 2.0 mmol) and H_4pdta (0.62 g, 2.0 mmol) were dissolved in water (15 mL) and stirred for one and a half hours. The pH value of the reaction mixture was adjusted to 6.5 with 5.0 M ammonium hydroxide, and heated at 70 °C for 12 hours. The mixture was standing at room temperature. Colorless crystalline materials were separated from the evaporated solution, which was washed with cold water and ethanol, and dried under vacuum. The yield was 61% (0.75 g). Anal. Found (calcd. for $C_{22}H_{60}La_2N_6O_{28}$): C, 23.4 (23.2); H, 5.1 (5.3); N, 7.2 (7.4). IR (KBr disk, /cm^{-1}): 3443_{vs}, 3243_{vs}, 2977_s, $\nu_{as}(CO_2)$, 1585_{vs}; $\nu_s(CO_2)$, 1408_{vs}, 1333_s, 1310_s, 1262_m; 1157_m, 1113_m, 1067_w, 1013_w, 986_w, 964_w, 931_m, 862_w, 772_m, 742_m, 703_m, 614_m, 568_m, 509_w, 439_w. Solution ^{1}H NMR (500 MHz, D_2O): δ (ppm) 3.311 (8H, s), 2.689 (4H, t, J = 5.0 Hz), 1.688 (2H, m); ^{13}C NMR (500 MHz, D_2O): δ (ppm) 182.7 (−**C**O_2), 65.1 (−**C**H_2CO_2), 62.2(−N**C**H_2−), 24.9 (−**C**H_2−). Preparation of cerium complex **2** was similar to that of **1**. The yield was 65% (0.74 g). Anal. Found (calcd. for $C_{22}H_{60}Ce_2N_6O_{28}$): C, 23.5 (23.2); H, 5.0 (5.3); N, 7.3 (7.4). IR (KBr disk, /cm^{-1}): 3439_s, 3221_s, $\nu_{as}(CO_2)$, 1589_{vs}; $\nu_s(CO_2)$, 1409_s, 1381_s, 1336_m, 1309_m; 1264_w, 1243_w, 1158_w, 1111_w, 1067_w, 1015_w, 985_w, 964_w, 928_m, 863_w, 776_w, 742_m, 706_w, 614_m, 564_w.

Preparations of $K_2[La_2(1,3\text{-pdta})_2(H_2O)_4]\cdot 11H_2O$ (3) and $K_2[Ce_2(1,3\text{-pdta})_2(H_2O)_4]\cdot 11H_2O$ (4)

$LaCl_3\cdot 7H_2O$ (0.74 g, 2.0 mmol) and H_4pdta (0.62 g, 2.0 mmol) were dissolved in water (15 mL) and stirred for one and a half hours. The pH value of the reaction mixture was adjusted to 6.5 with 5.0 M potassium hydroxide and heated at 70 °C for 12 hours. The mixture was standing in the air at room temperature. Colorless crystalline materials were separated from the evaporated solution, which was washed with cold water and ethanol, and dried under vacuum. The yield was 76% (0.94 g). Anal. Found (calcd. for $C_{22}H_{58}K_2La_2N_4O_{31}$): C, 21.4 (21.5); H, 4.7 (4.7); N, 4.5 (4.6). IR (KBr disk, /cm^{-1}): 3432_s, $\nu_{as}(CO_2)$, 1616_{vs}; $\nu_s(CO_2)$, 1409_s, 1391_s, 1336_s, 1301_m; 1262_m, 1157_w, 1124_w, 1075_w, 1024_w, 996_w, 931_m, 918_m, 876_m, 739_m, 607_m, 561_m, 424_w. Preparation of cerium complex **4** was similar to that of **3**. The yield was 69% (0.85 g). Anal. Found (calcd. for $C_{22}H_{58}K_2Ce_2N_4O_{31}$): C, 21.7 (21.4); H, 4.6 (4.7); N, 4.6 (4.5). IR (KBr disk, /cm^{-1}): 3388_s, $\nu_{as}(CO_2)$, 1589_{vs}; $\nu_s(CO_2)$, 1416_s, 1341_s, 1310_s, 1264_m; 1238_m, 1094_m, 1027_w, 991_w, 924_m, 879_w, 814_m, 723_s, 655_s, 532_m, 505_m, 447_w.

Preparation of $[La_2(1,3\text{-pdta})_2(H_2O)_4]_n\cdot[Sr_2(H_2O)_6]_n\cdot[La_2(1,3\text{-pdta})_2(H_2O)_2]_n\cdot 18nH_2O$ (5)

$(NH_4)_2[La_2(1,3\text{-pdta})_2(H_2O)_4]\cdot 8H_2O$ (**1**) (2.26 g, 2.0 mmol) was dissolved in water (20 mL) and stirred for one and a half hours. $Sr(NO_3)_2$ (0.85 g 4.0 mmol) was added to the solution and stirred at 70 °C for several minutes. The mixture was standing at 70 °C in sealed condition. Colorless crystalline materials were separated from the evaporated solution, which was washed with cold water and ethanol, and dried under vacuum. The yield was 68% (1.69 g). Anal. Found (calcd. for $C_{44}H_{116}La_4N_8O_{62}Sr_2$): C, 21.7 (21.4); H, 4.6 (4.7); N, 4.8 (4.5). IR (KBr disk, /cm^{-1}): 3426_s, 2955_m, 2853_m; $\nu_{as}(CO_2)$, 1581_{vs}; $\nu_s(CO_2)$, 1449_m, 1409_s; 1329_m, 1307_w, 1260_w, 1161_w, 1113_w, 1069_w, 1018_w, 989_w, 939_w, 868_w, 793_w, 718_m, 615_m, 567_w.

Catalytic reaction

The catalytic performance of the catalysts was investigated using a CH_4/O_2 = 2.8/1 mixture (molar ratio) as a reaction feed. OCM reaction for the investigated samples was carried out in a fixed-bed quartz tubular reactor (internal diameter 5 mm) at atmospheric pressure and a total flow rate of 50 mL·min^{-1}. The reactor was packed with 0.2 g samples (40-60 mesh sizes) between quartz wool plugs. The reactor was heated with a furnace connected to a temperature controller (Yudian AI-708PFKSL2). The performances of the catalysts were evaluated over the temperature range of 550-800 °C with a gas hourly space velocity (GHSV) of 15000 mL·g^{-1}·h^{-1}.

X-Ray crystallography

Suitable single crystals of **1**−**5** were selected and quickly mounted onto thin glass fibers to prevent the loss of water molecules. X-ray intensity data for complexes **2-5** were measured at 173 K (**1** was measured at 153 K) on a Oxford CCD diffractometer with Mo Kα radiation (λ = 0.71073 Å). Empirical adsorption was applied to all data using SADABS and CrysAlis (multi-scan) programs. The initial model was obtained through direct methods and the completion of the rest of the structure achieved by difference Fourier strategies. The structures were refined by least squares on F^2, with anisotropic displacement parameters for non-H atoms. Most of hydrogen atoms unambiguously defined by the stereochemistry were placed at their calculated positions and allowed to ride onto their host carbons both in coordinates as well as in thermal parameters (C–H, 0.97 Å). Those attached to oxygen and needed for the H-bonding description were located in a late Fourier map and refined with similarity restrains [O–H, 0.85(1) Å; H···H, 1.39(1) Å]. All calculations to solve and refine the structures and to obtain derived results were carried out with

the computer programs SHELXS 97, and SHELXL 97 programs. Full use of the CCDC package was also made for searching in the CSD Database.[14] CCDC deposition numbers are 974203−974207. Crystal data and structure refinements for **1**−**5** are summarized in Table 1.

Table 1 Crystal data and structural refinements for **1**−**5**.[a]

Compound reference	**1**	**2**	**3**	**4**	**5**
Chemical formula	$C_{22}H_{60}La_2N_6O_{28}$	$C_{22}H_{60}Ce_2N_6O_{28}$	$C_{22}H_{58}La_2N_4O_{31}K_2$	$C_{22}H_{58}Ce_2N_4O_{31}K_2$	$C_{44}H_{116}La_4N_8O_{62}Sr_2$
Formula Mass	1134.58	1137.00	1230.74	1233.16	2480.33
Crystal system	Triclinic				
a/Å	9.1820(2)	9.1815(4)	9.0362(3)	9.0204(5)	10.8949(3)
b/Å	10.7781(3)	10.7611(4)	10.8215(4)	10.7890(6)	14.4341(4)
c/Å	11.3519(3)	11.3292(4)	11.7411(3)	11.7467(5)	15.4414(5)
α/°	101.512(2)	101.806(3)	80.775(3)	80.869(4)	72.312(3)
β/°	105.284(2)	105.137(3)	80.888(2)	80.717(4)	71.264(3)
γ/°	100.003(2)	99.966(3)	76.343(3)	76.388(5)	76.982(2)
Unit cell volume/Å^3	1031.01(5)	1026.83(7)	1092.49(6)	1087.8(1)	2168.8(1)
Temperature/K	153(2)	173(2)			
Space group	$P\bar{1}$				
No. of formula units per unit cell, *Z*	1				
Radiation type	MoKα				
Absorption coefficient, *μ*/mm^{-1}	2.145	2.290	2.222	2.360	3.262
No. of reflections measured	10792	9075	9917	12971	29946
No. of independent reflections	5223	4252	4769	4979	9380
R_{int}	0.0397	0.0394	0.0280	0.0345	0.0586
Final R_1 values ($I > 2\sigma(I)$)	0.0294	0.0245	0.0262	0.0225	0.0390
Final $wR(F^2)$ values ($I > 2\sigma(I)$)	0.0698	0.0548	0.0639	0.0448	0.0710
Final R_1 values (all data)	0.0353	0.0285	0.0291	0.0281	0.0517
Final $wR(F^2)$ values (all data)	0.0723	0.0560	0.0653	0.0455	0.0753
Goodness of fit on F^2	0.938	1.025	1.020	1.002	1.051

[a] $R_1 = \Sigma||F_o| - |F_c|| / \Sigma|F_o|$, $wR_2 = \{\Sigma[w(F_o^2 - F_c^2)^2] / \Sigma[w(F_o^2)^2]\}^{1/2}$

Results and discussion

Syntheses of **1**−**5** were carried out in neutral aqueous solutions with different cations. In **1**−**4**, it is found that potassium salts combined with much more crystallized water molecules. When excess $Sr(NO_3)_2$ was added to the solution of **1**, a two-dimensinal coordination polymer $[La_2(1,3\text{-pdta})_2(H_2O)_4]_n \cdot [Sr_2(H_2O)_6]_n \cdot [La_2(1,3\text{-pdta})_2(H_2O)_2]_n \cdot 18nH_2O$ (**5**) was isolated in warm solution (70 °C) as shown in Scheme 1.

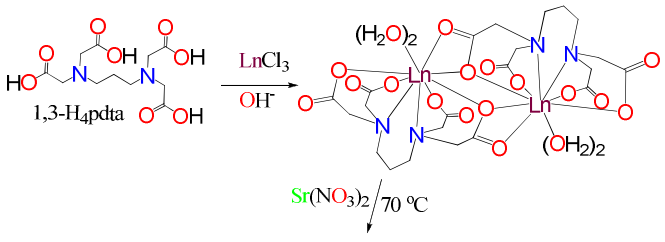

$[La_2(1,3\text{-pdta})_2(H_2O)_4]_n \cdot [Sr_2(H_2O)_6]_n \cdot [La_2(1,3\text{-pdta})_2(H_2O)_2]_n \cdot 18nH_2O$ (**5**)

Scheme 1 Preparations and conversions of 1,3-propanediaminetetraacetato lanthanides in different neutral solution (Ln = La or Ce).

Crystal structure descriptions

Figure 1 shows the anion structure of $(NH_4)_2[La_2(1,3\text{-pdta})_2(H_2O)_4] \cdot 8H_2O$ (**1**). Anion structures of **2**−**4** are similar to that of **1**, which are shown in Figures S1−S3.[§]

X-ray structural analysis revealed that dimeric complexes **1**−**4** have similar anion structures. Each Ln(III) cation exists in a decadentate coordination environment, which is different from those of usual nonadentate coordination in lanthanide ethylenediaminetetraacetates[7], and is also different from most of lanthanide propanediaminetetraacetates too. Here the flexible pdta ligand plays an important role to form the decadentate coordination environment. Usually, lanthanum or cerium ethylenediaminetetraacetates with rigid ethylene chain were often observed in nonadentate coordination number. Moreover, the type of lanthanide also plays a key role. Early lanthanides like La, Ce, Pr and Nd form decadentate coordination number easier than those of the heavy lanthanides with short ion radius due to lanthanide contraction. Pdta acts as a octadentate ligand. It uses two nitrogen atoms and four oxygen atoms of acetates to chelate one lanthanide ion. While one of the carboxy group forms a four-membered ring with the other lanthanum ion, forming a dimeric structure as shown in Figure 1.

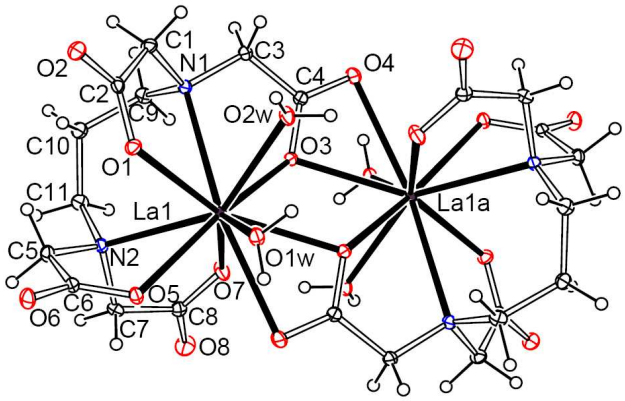

Figure 1 Anion structure of dimeric complex $(NH_4)_2[La_2(1,3\text{-pdta})_2(H_2O)_4] \cdot 8H_2O$ (**1**).

Molecular structure of $[La_2(1,3\text{-pdta})_2(H_2O)_4]_n\cdot[Sr_2(H_2O)_6]_n\cdot[La_2(1,3\text{-pdta})_2(H_2O)_2]_n\cdot 18nH_2O$ (**5**) is shown in Figure 2. In **5**, there are two kinds of lanthanum ions existed in different environments. The pdta ligand acts as ten-dentate and eleven-dentate ligand for two kinds of lanthanum ions respectively, which is unusual in pdta complexes. Two La1 ions, two 1,3-pdta ligands and two water molecules form a dimeric unit $La_2(1,3\text{-pdta})_2(H_2O)_2$ (unit 1), and two La2 ions, two 1,3-pdta ligands and four water molecules form another dimeric unit $La_2(1,3\text{-pdta})_2(H_2O)_4$ (unit 2), which is similar to that of the former dimeric complexes. As shown in Figure 3, we can clearly see this two kinds of dimeric lanthanum units. From Figure 2, we can see half of unit 1 still uses its two oxygen atoms of one carboxy group to coordinate with two strontium ions, and half of unit 2 uses its one carboxy group to chelate with the strontium and bridged with La1 of unit 1. Two strontium ions were bridged by coordinated water molecules (O6w). These make **5** forms a two dimensional coordination polymer.

As shown in Figure 4, the crystallied and coordinated water molecules form a thirty membered water molecules cluster. The water molecules were cleaved equally by one plane. These hydrogen bonds and the other hydrogen bonds between water molecules and carboxy oxygen atoms form two dimensional network extend to three dimensional supramolecular network as shown in Figure S4.

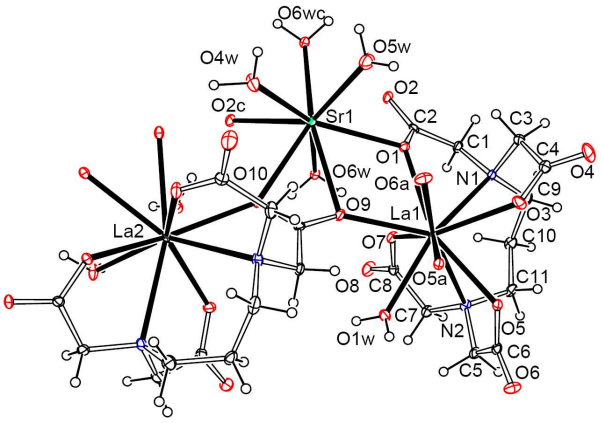

Figure 2 Molecular structure of $[La_2(1,3\text{-pdta})_2(H_2O)_4]_n\cdot[Sr_2(H_2O)_6]_n\cdot[La_2(1,3\text{-pdta})_2(H_2O)_2]_n\cdot 18nH_2O$ (**5**) in an asymmetric unit in 30% thermal ellipsoids.

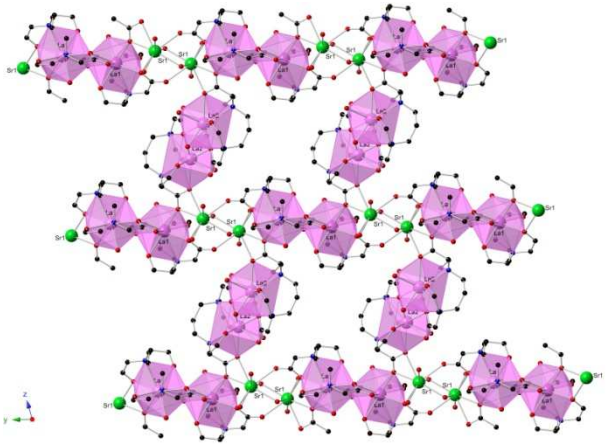

Figure 3 The infinite 2D structure of $[La_2(1,3\text{-pdta})_2(H_2O)_4]_n\cdot[Sr_2(H_2O)_6]_n\cdot[La_2(1,3\text{-pdta})_2(H_2O)_2]_n\cdot 18nH_2O$ (**5**).

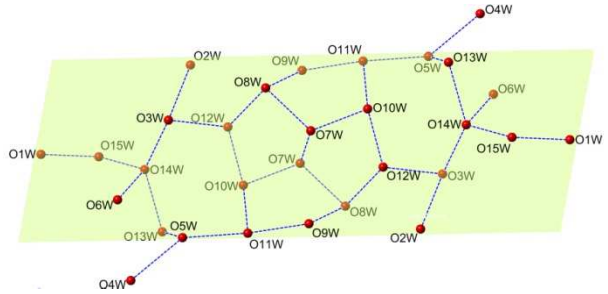

Figure 4 The coordinated and crystallized water molecules in $[La_2(1,3\text{-pdta})_2(H_2O)_4]_n\cdot[Sr_2(H_2O)_6]_n\cdot[La_2(1,3\text{-pdta})_2(H_2O)_2]_n\cdot 18nH_2O$ (**5**), forming a thirty water cluster.

Selected bond lengths for **1**–**5** are listed in Table 2. The average La–O bond length in dimeric **1** is 2.531(2) Å, and the bond lengths of the bridged four member ring are 2.591(2) and 2.773(2) Å. The average La–N and La–Ow bond lengths are 2.840(2) and 2.574(2) Å respectively. The corresponding bond lengths in lanthanum complexes **3** are 2.531(2), 2.589(2), 2.774(2), 2.832(2) and 2.584(2) Å. The two lanthanum complexes are very similar. The La–N bond lengths in **3** are shorter, while La–Ow are longer than those of **1**. In isomorphous cerium dimeric complexes **2** and **4**, the corresponding bond lengths are 2.506(2), 2.566 (2), 2.760(2), 2.827(2) and 2.552(2) Å for **2** and 2.509(2), 2.566 (2), 2.763(2), 2.817(2) and 2.570(2) Å for **4** respectively. Bond lengths in the two cerium complexes clearly demonstrate the lanthanide contraction effect. In complex **5**, for there are two kinds of lanthanum ions, the coordinate bonds must be divided into two kinds in order to show the features more clearly. La1 and La2 are both deca-coordinated. La1 ion has an average La1−O bond length [2.542(3) Å] for four oxygen atoms from one pdta ligand and 2.553(3) Å for La2 ion. When involving the bridged carboxy, there exist longer La1−O bond lengths [2.572(3), 2.672(3) and 2.779(3) Å] and longer La1−N bond lengths [2.864(4) Å]. For unit 2, the bond distance with only one water molecule is 2.504(3) Å. This is the shortest La–Ow bond in the five complexes.

NMR Analyses

Solution ^{13}C NMR spectra of **1** and H_4pdta are showed in Figure 5. The pH values of the solutions were around 6.4.

Solution ^{1}H NMR spectra are listed in Figures S5 and S6. When we compare ^{13}C NMR spectrum of **1** with that of H_4pdta, obvious downfield shifts show the coordination of pdta ligands. Only one set of ^{13}C NMR chemical shift data was observed for **1**. All carboxy groups give only one ^{13}C NMR siganl at 182.7 ppm ($\Delta\delta$ = 10.8 ppm) and one CH_2CO_2 signal at 65.1 ppm ($\Delta\delta$ = 6.3 ppm). Large downfield shifts were observed. From the molecular structure in solid state, there are two kinds of carboxy groups, but only one peak observed for carboxy groups in solution. This should result from the dissociation of the less strongly bridged carboxy group and form a monomeric species in the solution as shown in Scheme 2. There also only one set of signals with $-CH_2N-$ (62.2 ppm, $\Delta\delta$ = 6.4 ppm) and $-CH_2-$ (24.9 ppm, $\Delta\delta$ = 2.7 ppm). All in all, the bridged carboxy of pdta in dimeric lanthanum complexes must dissociate to monomeric unit.

The dissociation of dimeric complex to a monomeric in solution should mainly come from the less strongly bridged carboxy groups [La–$O_{\beta\text{-bridged}}$(av) 2.682(2), and 2.682(2) Å for dimeric lanthanum complexes **1** and **3**; 2.630(2) and 2.665(2) Å for **2** and **4** of dimeric cerium complexes], which are easy attacked and substituted by water molecules, comparing with the bond distances of normal coordinated β-carboxy groups [La–O(av) 2.531(2) and 2.531(2) Å for dimeric lanthanum complexes **1** and **3**; 2.506(2) and 2.509(2) Å for **2** and **4** of dimeric cerium complexes].

Table 2. Selected bond lengths (Å) for **1**–**4** and **5.**

Compound entry	Ln–$O_{\beta\text{–carboxy}}$(av)	Ln–$O_{\beta\text{-bridged}}$	Ln–N(av)	Ln–Ow (av)
1	2.531(2)	2.591(2), 2.773(2)	2.840(2)	2.574(2)
2	2.506(2)	2.566(2), 2.760(2)	2.827(2)	2.552(2)
3	2.531(2)	2.589(2), 2.774(2)	2.832(2)	2.584(2)
4	2.509(2)	2.566(2), 2.763(2)	2.817(2)	2.570(2)
5-unit 1	2.542(3)	2.572(3), 2.672(3), 2.779(3)	2.864(4)	2.504(3)
5-unit 2	2.555(3)	2.644(3), 2.696(3)	2.861(4)	2.557(3)
		Sr–$O_{\beta\text{-bridged}}$(av)		Sr–Ow (av)
5-Sr	–	2.663(3)	–	2.584(3)

In ^{1}H NMR spectrum of H_4pdta (Fig. S5), the eight acetate protons are equivalent and result in one signal at 4.061 ppm. The four $-CH_2N-$ protons are equivalent and result in a triple signal centred at 3.433 ppm and the two protons of $-CH_2-$ give a penta-signal centred at 2.249 ppm. When we compare the ^{1}H NMR spectra between H_4pdta and lanthanum complex **1**, we find out that they give only one set of signal assigned to different $-CH_2-$ groups, which is consistent with the ^{13}C NMR spectra. 3.311 (8H, s), 2.689 (4H, t, J = 5.0 Hz), 1.688 (2H, m); Through the ^{1}H NMR spectrum of **1** (Fig. S6), a singlet at 3.311 ppm (8H, s, $\Delta\delta$ = –0.750 ppm) for acetate protons and a tri-signal centred at 2.689 ppm (4H, t, J = 7.5 Hz, $\Delta\delta$ = –0.744 ppm) for the $-CH_2N-$ protons and multiple peaks centred at 1.688 (2H, m, $\Delta\delta$ = –0.561 ppm). There are big shifts of $\Delta\delta$ values for **1**. This is also an indication for the strong coordination of 1,3-pdta ligand in **1**. Morever, these also indicate the dissociation of bridged carboxy groups in **1**. This is because that only one set of signal was observed for $-CO_2-$, $-CH_2CO_2$, $-CH_2N-$ and $-CH_2-$ groups. The result is consistent with ^{13}C NMR measurements.

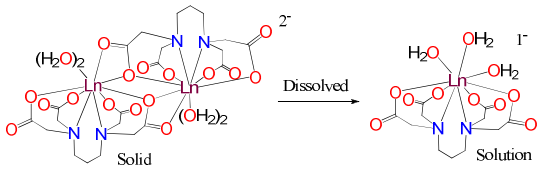

Scheme 2 Conversions of dimeric 1,3-propanediaminetetraacetato lanthanides to monomers when dimeric complexes were dissolved in water.

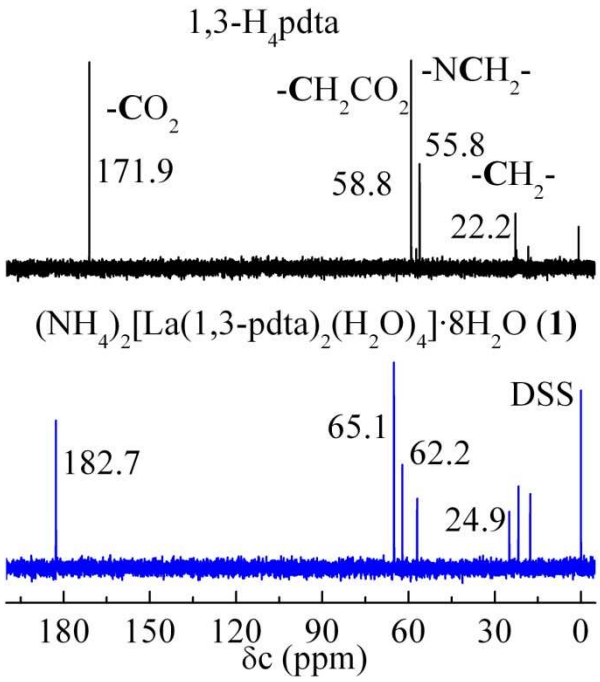

Figure 5 Solution ^{13}C NMR spectra of 1,3-H_4pdta and $(NH_4)_2[La_2(1,3\text{-pdta})_2(H_2O)_4]\cdot 8H_2O$ (**1**).

Vibrational Spectra

IR vibrational spectra of **1**–**5** are listed in Figures S7–S11. In the region between 1616 and 1581 cm^{-1} and between 1449 and 1330 cm^{-1}, complex **1**–**5** gives two typical bands correspond to the bounded carboxy groups $\nu_{as}(COO^-)$ and $\nu_s(COO^-)$, respectively. The value of $[\nu(COO^-)_{as} - \nu(COO^-)_s]$ is about 173

cm^{-1} in **1** suggests that the coordination of the carboxy groups is most probably of the bridging type.[15] This is also observed for complexes **2**–**4**. In **5**, the value of $[\nu(COO^-)_{as} - \nu(COO^-)_s]$ is about 132 cm^{-1} suggests the chelate type of 1,3-pdta ligand. This is consistent with the structural analysis which shows more chelate bonds in 1,3-pdta ligands. The changes confirm that the oxygen atoms from the carboxy groups of 1,3-pdta coordinated with the centre ions. The ν(C–N) of complexes **1**–**5** near 1100 cm^{-1} displays obvious blue-shift compared with that of H_4pdta, suggesting that nitrogens of pdta are coordinated to centre ions.

Thermogravimetric analyses (TGA)

Thermal stability and decomposition patterns of the complexes were investigated by thermo-gravimetric analyses. The TG-DTG curves of complexes **1** and **5** are listed in Figure S12 and Figure 6. The first part of big weight loss starts at 80 and 94 °C, which correspond to the loss of crystallized water molecules for **1** and **5** respectively. The coordinated water molecules decompose at 120, 144 and 192°C for **1** and **5**. Then the weight keeps steady. The biggest weight loss starts from 299 and 366 °C for **1** and **5** respectively, where the ligand is decomposed step by step in this process. At 690 and 731°C, there is a small weight loss, which may corresponds to the conversion of lanthanum oxocarbonate to lanthanun oxide for **1** and **5** respectively (Figures 6 and S12), the latter shows strong interaction with strontium. At last, there exist a small weight loss around 850 °C, which is assigned for the thermal decomposition of strontium carbonate for $[La_2(1,3\text{-pdta})_2(H_2O)_4]_n[Sr_2(H_2O)_6]_n[La_2(1,3\text{-pdta})_2(H_2O)_2]_n{\cdot}18nH_2O$ (**5**).

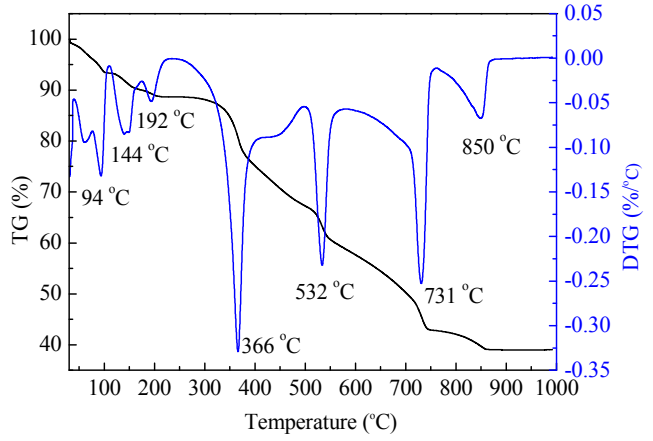

Figure 6 TG-DTG curves of $[La_2(1,3\text{-pdta})_2(H_2O)_4]_n{\cdot}[Sr_2(H_2O)_6]_n{\cdot}[La_2(1,3\text{-pdta})_2(H_2O)_2]_n{\cdot}18nH_2O$ (**5**)

Characterization of lanthanum and strontium lanthanum catalysts

Complexes **1** and **5** were calcinated under atmosphere at 600 °C for 6 hours to obtain the final catalysts. The X-ray diffraction patterns of the samples before and after reacion are shown in Figure 7. Before reaction, diffraction peaks were assigned to lanthanum oxocarbonate $La_2O_2CO_3$ (PDF# 84-1963) for **1**. While the diffraction peaks were assigned to the mixture of La_2O_3 (PDF# 74-2430), $SrCO_3$ (PDF# 84-1778) and $La_2O_2CO_3$ (PDF# 84-1963) for **5**. The two thermal decomposition products contain carbonates. This is because the alkaline nature of the centre ions, and the coordinated carboxy groups increase the alkalescence, which is consistent with the results of thermogravimetric analyses. In addition, the intensity of product from **5** decreased obviously and the width became broaden compared with that of **1**, which indicated that the particle sizes from **5** decreased. After the reaction, there are no obvious changes for **1**, this indicated that lanthanum oxocarbonate from **1** is relatively stable. While the intensities of La_2O_3 (PDF# 74-2430) increased and the widths of the peaks narrowed for **5**, this showed that the particle sizes from **5** increased obviously after reaction. Moreover, the intensities of lanthanum oxocarbonate $La_2O_2CO_3$ weakened, which means the ammount of $La_2O_2CO_3$ decreased.

The SEM images of the products from **1** and **5** are shown in Figure 8 before and after the reactions. As shown in the images, the morphology of lanthanum oxocarbonate from **1** is in rod-like shape after decomposition, while that from **5** is graininess, and particle sizes from **5** are samller than that from **1**, which is consistent with the XRD results. After the reaction, the morphology of lanthanum oxocarbonate from **1** also keeps in rod-like shape, but not so uniform. While there are a lot of agglomerations for **5**, and the particle sizes grow up obviously.

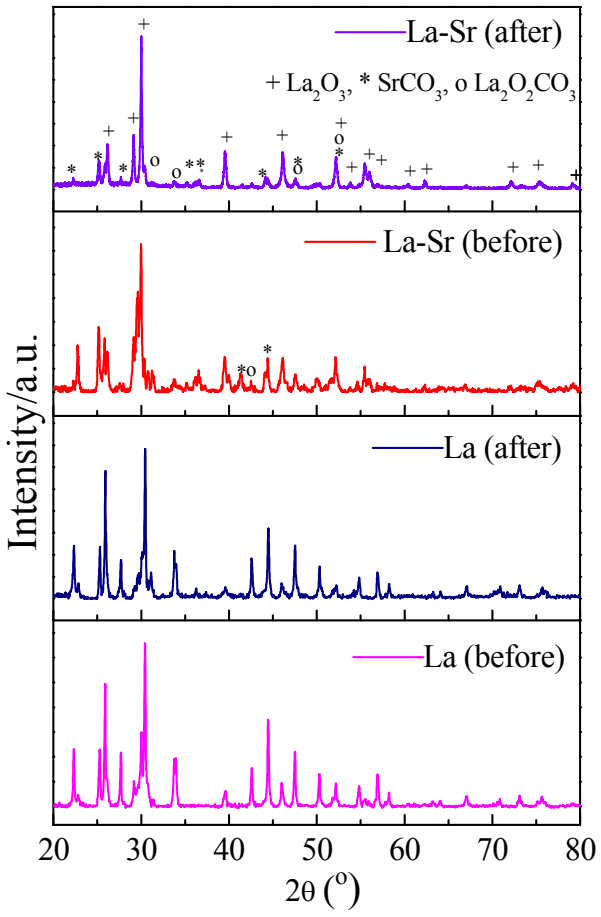

Figure 7 The X-ray diffraction patterns of the thermal decomposition products from $(NH_4)_2[La_2(1,3\text{-pdta})_2(H_2O)_4]\cdot 8H_2O$ (**1**) and $[La_2(1,3\text{-pdta})_2(H_2O)_4]_n\cdot[Sr_2(H_2O)_6]_n\cdot[La_2(1,3\text{-pdta})_2(H_2O)_2]_n\cdot 18nH_2O$ (**5**) (before and after catalytic reactions).

Catalytic activities for oxidative coupling of methane (OCM)

As shown in Figure 9, the catalytic performances of the thermal decomposition products from **1** and **5** for OCM reactions were performed at the temperatures ranging from 550 to 800 °C. The detail catalytic activity data were shown in Table S1. At 550 °C, there is no conversion of methane for lanthanum oxocarbonate from **1**, While the conversion of methane and selectivity to C_2 are 12.6% and 24.1% respectively for **5**. The catalytic performances increased rapidly with the increase of the temperature. At 700 °C, the conversion of methane and the selectivity to C_2 reach 23.0% and 45.8% for lanthanum oxocarbonate from **1**, which are much better than that of conventional bulk La_2O_3.[16] For **5**, the conversion of methane and selectivity to C_2 are 29.7% and 51.7% respectively at 750 °C, which are also better than that of bulk La-Sr sample.[17] In addition, the catalytic performances for the thermal product from **5** are much better than that of lanthanum oxocarbonate from **1**. This may be attributed to decrease of the particle sizes, which can be observed in SEM images (Figure 2), and increase of the alkaline sites as the addition of strontium. This is in consistent with the previous reported results that alkaline earth oxide especially strontium had an excellent promoted effect on the La_2O_3 catalytic activity for OCM reaction,[18] while the OCM catalytic performance of lanthanum oxocarbonate from **1** is interesting.

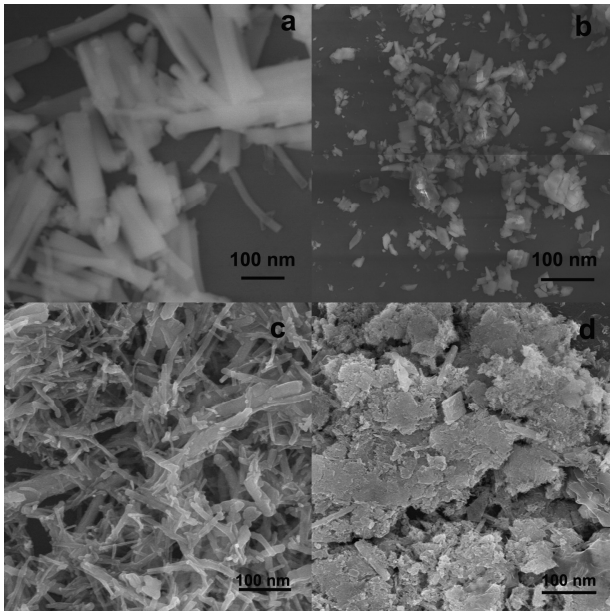

Figure 8 The SEM images of the calcinated products from **1** and **5**. a, The thermal decomposition product from **1**; b, The thermal decomposition product from **5**; c, the thermal decomposition product of **1** after catalytic reaction; d, the thermal decomposition product of **5** after catalytic reaction.

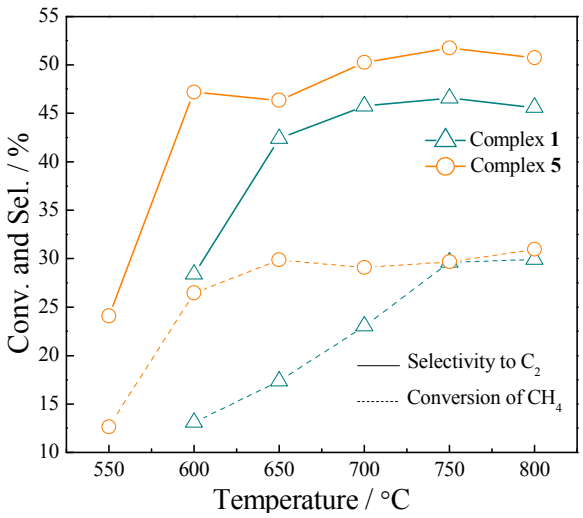

Figure 9 Catalytic activity for oxidative coupling of methane for the thermal decomposition products from **1** and **5**. (CH_4/O_2 = 2.8/1, GHSV = 15000 $mL\cdot g^{-1}\cdot h^{-1}$).

Conclusions

In summary, four dimeric 1,3-propanediaminetetraacetato lanthanide complexes $(NH_4)_2[Ln_2(1,3\text{-pdta})_2(H_2O)_4]\cdot 8H_2O$ [Ln = La, **1**; Ce, **2**] and $K_2[Ln_2(1,3\text{-pdta})_2(H_2O)_4]\cdot 11H_2O$ [Ln = La, **3**; Ce, **4**] and a novel two-dimensional strontium 1,3-propanediaminetetraacetato lanthanum complex (**5**) were isolated and characterized. The thermal decomposition products from **1** and **5** show good catalytic activities for the reaction of oxidative coulping of methane. Strontium had an excellent promoted effect, and lanthanum oxocarbonate also shows an interesting result on the catalytic reaction.

Acknowledgements

This work was financially supported by the National Science Foundation of China (21133007, 21033006, 21373169), the Ministry of Science and Technology of China (2010CB732303, 2012CB214900) and PCSIRT(No.IRT1036).

Notes and references

State Key Laboratory of Physical Chemistry of Solid Surfaces, College of Chemistry and Chemical Engineering, Xiamen University, Xiamen, 361005, China, Fax: +86 592 2183047; Tel: +86 592 2184531; E-mail: zxcao@xmu.edu.cn, zhzhou@xmu.edu.cn

† Electronic Supplementary Information (ESI) is available including Ortep figures of **2**−**4** (Fig. S1−S3), 3D supramolecular network of **5** (Fig. S4); Solution ^{1}H NMR spectra of H_4pdta and **1** (Figs. S5 and S6); IR vibrational spectra (Figs. S7−S11); TG-DTG curves of **1** (Fig. S12) and the catalytic activities data (Table S1). For ESI and crystallographic data in CIF or other electronic format see DOI: 10.1039/b000000x/

1. (a), J. Yang, Q. Yuo, G. D. Li, J. J. Cao, G. H. Li and J. S. Chen, *Inorg. Chem.*, 2006, **45**, 2857-2865; (b), X.-L. Li, C.-L. Chen, H.-P. Xiao, A.-L. Wang, C.-M. Liu, X. Zheng, L.-J. Gao, X.-G. Yang and S.-M. Fang, *Dalton Trans.*, 2013, **42**, 15317-15325; (c), J. Tian, B. Li, X. Zhang, X. Li, X. Li and J. Zhang, *Dalton Trans.*, 2013, **42**,

8504-8511; (d), C. Benelli and D. Gatteschi, *Chem. Rev.*, 2002, **102**, 2369-2387.

2. (a), I. Hemmila and V. Laitala, *J. Fluoresc.*, 2005, **15**, 529-542; (b), M. Elhabiri, R. Scopelliti, J. C. G. Bunzli and C. Piguet, *J. Am. Chem. Soc.*, 1999, **121**, 10747-10762; (c), C. Piguet, J. C. G. Bunzli, G. Bernardinelli, G. Hopfgartner, S. Petoud and O. Schaad, *J. Am. Chem. Soc.*, 1996, **118**, 6681-6697.
3. (a), S. Shirvani-Arani, S. J. Ahmadi, A. Bahrami-Samani and M. Ghannadi-Maragheh, *Anal. Chim. Acta*, 2008, **623**, 82-88; (b), Y. Zhao, L.-L. Liang, K. Chen, T. Zhang, X. Xiao, Y.-Q. Zhang, Z. Tao, S.-F. Xue and Q.-J. Zhu, *Crystengcomm*, 2013, **15**, 7987-7998; (c), C. Y. Li, J. Z. Gao, W. Yang, B. Y. Li and H. T. Liu, *Rare Metals*, 2000, **19**, 136-140; (d), H. L. Nekimken, B. F. Smith, G. D. Jarvinen and C. S. Bartholdi, *Solvent Extr. Ion Exc.*, 1992, **10**, 419-429.
4. (a), J. C. G. Bunzli, *Accounts Chem. Res.*, 2006, **39**, 53-61; (b), M. Bottrill, L. K. Nicholas and N. J. Long, *Chem. Soc. Rev.*, 2006, **35**, 557-571; (c), J. A. Peters, J. Huskens and D. J. Raber, *Prog. Nucl. Mag. Res. Sp.*, 1996, **28**, 283-350; (d), D. H. Powell, O. M. NiDhubhghaill, D. Pubanz, L. Helm, Y. S. Lebedev, W. Schlaepfer and A. E. Merbach, *J. Am. Chem. Soc.*, 1996, **118**, 9333-9346.
5. (a), A. L. Kustov, O. P. Tkachenko, L. M. Kustov and B. V. Romanovsky, *Environ. Int.,* 2011, **37**, 1053-1056; (b), A. Rath, E. Aceves, J. Mitome, J. Liu, U. S. Ozkan and S. G. Shore, *J. Mol. Catal. A-Chem.*, 2001, **165**, 103-111; (c), T. Mirkovic, M. A. Hines, P. S. Nair and G. D. Scholes, *Chem. Mater.*, 2005, **17**, 3451-3456; (d), T. J. Boyle, R. Raymond, D. M. Boye, L. A. M. Ottley and P. Lu, *Dalton Trans.*, 2010, **39**, 8050-8063; (e), D. Liu and D. Cui, *Dalton Trans.*, 2011, **40**, 7755-7761; (f), S. Mishra, G. Ledoux, E. Jeanneau, S. Daniele and M.-F. Joubert, *Dalton Trans.*, 2012, **41**, 1490-1502; (g), A. J. Wooles, D. P. Mills, W. Lewis, A. J. Blake and S. T. Liddle, *Dalton Trans.*, 2010, **39**, 500-510.
6. (a), K. Kili, L. Hilaire and F. Le Normand, *Phys. Chem. Chem. Phys.*, 1999, **1**, 1623-1631; (b), N. B. Wong, K. C. Tin, Q. N. Zhu, M. Z. Zhang and X. Q. Qiu, *J. Chem. Technol. Biot.*, 1996, **67**, 164-168; (c), Y. Guo, G. Lu, Z. Zhang, S. Zhang, Y. Qi and Y. Liu, *Catal. Today*, 2007, **126**, 296-302.
7. (a), A. G. Dedov, G. D. Nipan, A. S. Loktev, A. A. Tyunyaev, V. A. Ketsko, K. V. Parkhomenko and I. I. Moiseev, *Appl. Catal. A-Gen.*, 2011, **406**, 1-12; (b), L. Qiu, T. Ichikawa, A. Hirano, N. Imanishi and Y. Takeda, *Solid State Ionics*, 2003, **158**, 55-65; (c), W. Wang, C. Su, R. Ran and Z. Shao, *J. Power Sources*, 2011, **196**, 3855-3862; (d), A. Goel, A. A. Reddy, M. J. Pascual, L. Gremillard, A. Malchere and J. M. F. Ferreira, *J. Mater. Chem.*, 2012, **22**, 10042-10054.
8. (a), B. J. Clapsaddle, B. Neumann, A. Wittstock, D. W. Sprehn, A. E. Gash, J. H. Satcher, Jr., R. L. Simpson and M. Baeumer, *J. Sol-Gel Sci. Techn.*, 2012, **64**, 381-389; (b), J. P. Boilot, T. Gacoin and S. Perruchas, *C.R. Chim.*, 2010, **13**, 186-198; (c), Q. Kuang, Z.-W. Lin, W. Lian, Z.-Y. Jiang, Z.-X. Xie, R.-B. Huang and L.-S. Zheng, *J. Solid State Chem.*, 2007, **180**, 1236-1242; (d), L. Armelao, G. Bottaro, G. Bruno, M. Losurdo, M. Pascolini, E. Soini and E. Tondello, *J. Phys. Chem. C*, 2008, **112**, 14508-14512.
9. M. L. Panchula and M. Akinc, *J. Eur. Ceram. Soc.*, 1996, **16**, 833-841.
10. (a), P. Ji, M. Xing, S. Bagwasi, B. Tian, F. Chen and J. Zhang, *Mater. Res. Bull.*, 2011, **46**, 1902-1907; (b), G. Jia, C. Zhang, L. Wang, S. Ding and H. You, *J. Alloy. Compd.*, 2011, **509**, 6418-6422; (c), F. Chen, Y.-J. Zhu, K.-W. Wang and Y.-B. Pan, *Curr. Nanosci.*, 2009, **5**, 266-272.
11. (a), S. Sohn, Y. Kwon, Y. Kim and D. Kim, *Powder Technol.*, 2004, **142**, 136-153; (b), Happy, A. I. Y. Tok, L. T. Su, F. Y. C. Boey and S. H. Ng, *J. Nanosci. Nanotechno.*, 2007, **7**, 907-915; (c), J. G. Li, T. Ikegami, T. Mori and Y. Yajima, *J. Mater. Res.*, 2003, **18**, 1149-1156.
12. (a), G. O. Siqueira, A. d. O. Porto, M. M. Viana, H. V. da Silva, Y. G. de Souza, H. W. Alves da Silva, G. M. de Lima and T. Matencio, *Phys. Chem. Chem. Phys.*, 2013, **15**, 16236-16241; (b), I. Melian-Cabrera, M. L. Granados and J. L. G. Fierro, *Phys. Chem. Chem. Phys.*, 2002, **4**, 3122-3127; (c), G. A. A. Costa, M. C. Silva, A. C. B. Silva, G. M. de Lima, R. M. Lago and M. T. C. Sansiviero, *Phys. Chem. Chem. Phys.*, 2000, **2**, 5708-5711; (d), M. F. Pinheiro da Silva, F. M. de Souza Carvalho, T. d. S. Martins, M. C. de Abreu Fantini and P. C. Isolani, *J. Therm. Anal. Calorim.*, 2010, **99**, 385-390; (e), L. Si, L. Yue and D. Jin, *Cryst. Res. Technol.*, 2011, **46**, 1149-1154.
13. M.-L. Chen, Y.-C. Guo, F. Yang, J.-X. Liang, Z.-X. Cao and Z.-H. Zhou, *Dalton Transactions*, 2014, 10.1039/C3DT52837E.
14. (a), G. M. Sheldrick, *SHELXS-97, SHELXL-97, and SHELXTL/PC, Programs for solution and refinement of crystal structures*, University of Göttingen, Göttingen, 1997; (b), A. J. C. Wilson, *International Tables for Crystallography*, 1995.
15. K. Nakamoto, *Infrared and Raman Spectra of Inorganic and Coordination Compounds: Part B., Applications in Coordination, Organometallic, and Bioinorganic Chemistry*, John Wiley & Sons, Inc., New Jersey, 2009.
16. H. L. Wan, X. P. Zhou, W. Z. Weng, R. Q. Long, Z. S. Chao, W. D. Zhang, M. S. Chen, J. Z. Luo and S. Q. Zhou, *Catal. Today*, 1999, **51**, 161-175.
17. R. Q. Long, Doctoral Dissertation, Xiamen University, 1997.
18. V. R. Choudhary, S. A. R. Mulla and V. H. Rane, *J. Chem. Technol. Biot.*, 1998, **72**, 125-130.

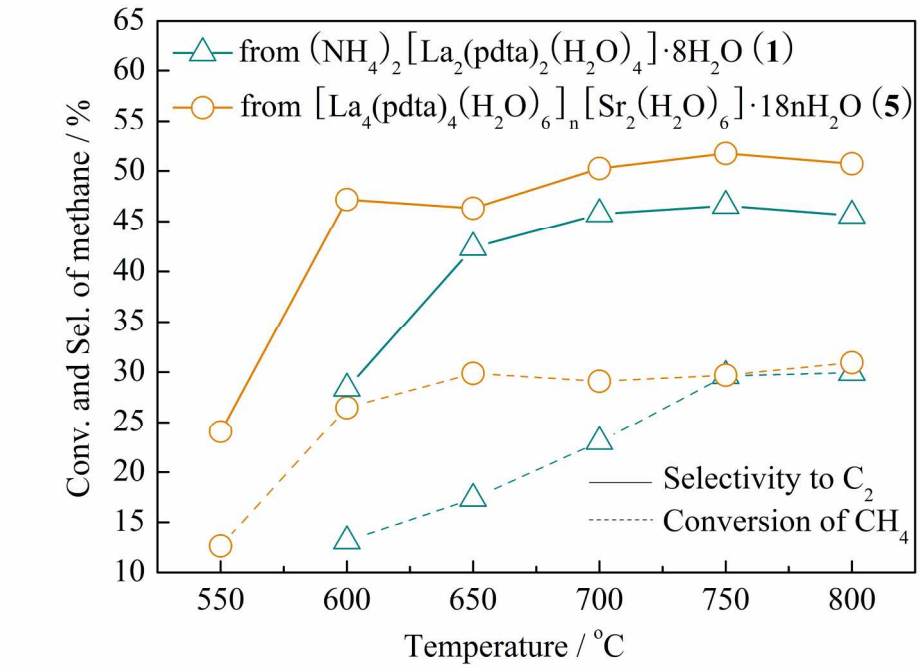

1,3-propanediaminetetraacetato lanthanides as the precursors of catalysts for the oxidative coupling of methane, where the precursors were fullly characterized by spectral and structural analyses.
205x162mm (300 x 300 DPI)